

See discussions, stats, and author profiles for this publication at: <https://www.researchgate.net/publication/11291269>

Location of protons in anhydrous Keggin heteropolyacids $H(3)PMo(12)O(40)$ and $H(3)PW(12)O(40)$ by $(1)H[(31)P]/(31)P[(1)H]$ REDOR NMR and DFT quantum chemical calculations.

ARTICLE *in* JOURNAL OF THE AMERICAN CHEMICAL SOCIETY · AUGUST 2002

Impact Factor: 12.11 · Source: PubMed

CITATIONS

21

READS

44

6 AUTHORS, INCLUDING:



Michel Guelton

Université des Sciences et Technologies de Li...

56 PUBLICATIONS 1,100 CITATIONS

SEE PROFILE

Location of Protons in Anhydrous Keggin Heteropolyacids $\text{H}_3\text{PMo}_{12}\text{O}_{40}$ and $\text{H}_3\text{PW}_{12}\text{O}_{40}$ by $^1\text{H}\{^{31}\text{P}\}/^{31}\text{P}\{^1\text{H}\}$ REDOR NMR and DFT Quantum Chemical Calculations

S. Ganapathy,^{†,‡} M. Fournier,[§] J. F. Paul,[§] L. Delevoye,[⊥] M. Guelton,[§] and J. P. Amoureux^{*,‡}

Contribution from the National Chemical Laboratory, 411 008 Pune, India, LCPS, CNRS-8012, Université de Lille1, 59655 Villeneuve d'Ascq, France, Laboratoire de Catalyse, CNRS-8010, Université de Lille1, 59655 Villeneuve d'Ascq, France, and Bruker-France, 67166 Wissembourg, France

Received December 21, 2001

Abstract: HeteroPolyAcids (HPA's) are a class of solid acids that have broad applications in many fields of science and technology, including catalysis and chemical engineering. The proton locations within the thermally stable and commonly known Keggin unit, which is the primary structure building unit/block, has remained undetermined in anhydrous HPAs, despite numerous theoretical and experimental efforts. However, Rotational Echo DOuble Resonance (REDOR) NMR and Density Functional Theory (DFT) quantum chemical calculations offer a new opportunity to determine the exact locations of protons within the Keggin unit. The crucial experimental evidence is provided for the basic and very extensively studied acidic form of $\text{H}_{8-n}\text{X}^{n+}\text{M}_{12}\text{O}_{40}$, X = Si, P and M = Mo, W, belonging to the Keggin structure. While showing that the acidic protons are located in the bridging oxygen positions ($R_{\text{P-H}} = 520 \pm 20$ pm) in $\text{H}_3\text{PMo}_{12}\text{O}_{40}$ and in the terminal oxygen positions ($R_{\text{P-H}} = 570 \pm 20$ pm) in $\text{H}_3\text{PW}_{12}\text{O}_{40}$, REDOR measurements also provide for the first time the structural basis to consistently rank the acid strength for the important class of Keggin solid catalysts.

I. Introduction

Due to their versatile properties, iso- and heteropolycompounds have received much attention for many years.^{1,2} Among the numerous molecular structures, which are now reported, often with crystal data,^{3,4} heteropolymolybdates and tungstates related to the well-known Keggin structure received the most attention. These dodecamolybdo(tungsto) phosphate (silicate, germanate, or arsenate) $\text{X}^{n+}\text{M}_{12}\text{O}_{40}^{(8-n)-}$ compounds can be isolated either as acidic forms or salts. Studied for a long time because of their analytical properties (color of their reduced compounds, slight solubility of their alkylammonium salts or protein combination, reversible multisteps of electron exchange, ...), Keggin heteropolycompounds are now extensively used in catalysis.^{5–10} Presently, four industrial processes include het-

eropolycompounds: propylene hydration, methacroleine and olefin oxidation, and polymerization of tetrahydrofuran.¹¹

The reason of this particular interest seems related to their bifunctional behavior: acidic and redox. From this point of view, heteropolycompounds are expected to exhibit a very good selectivity. However, an adequate linkage between the polyoxometalate properties and the reaction conditions is needed that distinguishes homogeneous and heterogeneous catalysis. For the former, the properties of the Keggin ions in solutions can be reasonably used to choose the most appropriate catalyst. For example, in acidic catalysis the Hammett function can be used and in oxidation reactions the apparent standard redox potential seems rather adequate. It seems interesting to remark that, except for the methacroleine oxidation, industrial processes are based on polyoxometalate homogeneous catalysis with high conversion and selectivity at very low temperature. In the solid–gas reaction the problem is quite different, and it is important to consider the bulk properties and the surface behavior. Many results have been previously reported on the acidic properties in the solid state of the dodecamolybdo(tungsto)phosphoric acids, $\text{H}_3\text{PMo}_{12}\text{O}_{40}$ or $\text{H}_3\text{PW}_{12}\text{O}_{40}$ (abbreviated as PMo or PW, respectively), and many promising reactions are nowadays studied: alcohol dehydration, alkylation, isomerization, oxy-

* To whom correspondence should be sent. E-mail: jean-paul.amoureux@univ-lille1.fr.

[†] National Chemical Laboratory.

[‡] LCPS, Université de Lille1.

[§] Laboratoire de Catalyse, Université de Lille1.

[⊥] Bruker-France.

(1) Souchay, P. *Ions minéraux condensés*; Masson: Paris, 1969.

(2) Pope, M. T. *Heteropoly and isopoly oxometalates*; Springer-Verlag: Berlin, 1983.

(3) Weakley, T. J. R. *Struct. Bonding* **1974**, 18, 131.

(4) Evans, H. T., Jr. Heteropoly and isopoly complexes of the transition elements of groups 5 and 6. In *Perspect. Struct. Chem.* **1971**, 4, 1.

(5) Okura, T.; Mizuno, N.; Misono, M. *Adv. Catal.* **1996**, 41, 113.

(6) Mizuno, N.; Misono, M. Heteropolyanions in catalysis. In *J. Mol. Catal. A: Chem.* **1994**, 86 (special issue), 319.

(7) Mizuno, N.; Misono, M. *Chem. Rev.* **1998**, 98, 199.

(8) Kozhevnikov, I. V. *Chem. Rev.* **1998**, 98, 171.

(9) Hill, C. L., Ed. Polyoxometalates in Catalysis. In *J. Mol. Catal. A* **1996**, 114 (special issue), 1–3.

(10) Hill, C. L.; Prosser-McCarthy, C. M. *Coord. Chem. Rev.* **1995**, 143, 407.

(11) Misosno, M.; Nojiri, N. *Appl. Catal.* **1990**, 64, 1.

dehydrogenation,^{5–7} In both acidic and oxidative processes some acid centers are needed. The acidic behavior of HeteroPolyAcids (HPAs) is now understood in homogeneous catalysis and it is well-known that Keggin units are then essentially completely dissociated. On the contrary, in high-temperature solid-state heterogeneous catalysts, the proton site location, which is of fundamental interest, is most of the time unknown.

The basic Keggin unit is composed of a central XO_4 tetrahedron ($X = P$ or Si) surrounded by 12 MO_6 octahedra ($M = Mo$ or W). It is now well-established that Keggin HPAs can be isolated from aqueous solutions, in different hydrated crystals depending mainly on the temperature and slightly on the acidic conditions. Fully hydrated compounds with a cubic lattice (29–30 H_2O per Keggin unit) are obtained at very low temperatures. However, these compounds quickly evolve at room temperature to the $13H_2O$ hydrate with a triclinic lattice. In these solids, protons are trapped in polyhydroxonium $H_5O_2^+$ ions through hydrogen bonds with the oxygen atoms of Keggin ions. In hydrated forms, HPAs possess a discrete ionic structure comprised of fairly mobile basic structural units, which exhibit extremely high proton mobility. However, at higher temperature, close to 300 °C, which is the usual temperature of many heterogeneous reactions, water molecules leave the lattice and hydrogen atoms have to be bound to the polyanion.¹² In these conditions, the Bronsted acidic properties of the solid depend strongly on the electrical charge of the oxygen atoms on which protons are attached. That is a major problem for catalysis and some attempts to localize these protons have previously been reported.^{13,14} Unfortunately, the results remain ambiguous, especially for the molybdenum compounds, which are the most promising catalysts due to their bifunctional properties. It now seems that, in mild oxidation, the selectivity depends on the type of oxygen atoms and on their mobility. So, the capability of creating oxygen vacancies, through water removal, depends on the proton location too. On the other hand, the thermal stability of HPAs depends strongly on the water evolution and many results are reported about the effects of some new supports for increasing the HPA stability. As it now seems that the interaction between the Keggin anion and the support occurs through shared protons, determining the HPA protonation sites has become mandatory. However, due to the difficulties of obtaining good single crystals suitable for X-ray diffraction, and to the fact that protons are nearly not “visible” with this technique, proton locations are only known for a few HPAs in partly hydrated form. Indeed, when removing water molecules, crystals evolve to poorly crystallized or even amorphous materials. Determination of proton location in anhydrous HPAs thus implies using spectrometric investigations. However, even if the Keggin anions exhibit very well-defined vibration patterns,¹⁵ some of the fundamental stretching bands are mixed and it is never possible to prove the oxygen atoms linked to

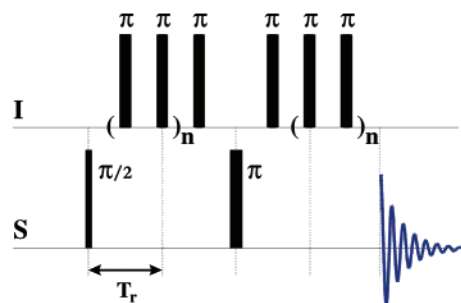


Figure 1. REDOR pulse sequence with a spin-echo on the observed (S) nuclei (1H or ^{31}P) and dephasing π pulses on the corresponding I spins (^{31}P or 1H). For a given value of $N = 2(n + 1)$, two experiments are performed: one with the π pulses on I ($S(NT_r)$ experiment) and one without these pulses ($S_0(NT_r)$ experiment). The REDOR fraction, $[S_0(NT_r) - S(NT_r)]/S_0(NT_r) = \Delta S/S_0$, is measured as a function of NT_r , where T_r is the rotor period.

the protons. In addition, considering the very similar electronegativities of molybdenum and tungsten atoms, metal–oxygen bonds are expected to have identical ionic character leading to molybdenum and tungsten Keggin-type HPAs that should have very similar acidic properties, except if the protonation sites are different.

The present study is therefore focused on the determination of proton location in the anhydrous heteropolyacids $H_3PMo_{12}O_{40}$ and $H_3PW_{12}O_{40}$ through $^1H\{^{31}P\}$ and $^{31}P\{^1H\}$ Rotational Echo Double Resonance (REDOR) NMR experiments, correlated with “ab initio” DFT calculations.

II. Experimental Section

Catalyst Preparation. Hydrated HPAs were prepared according to a method previously described.¹⁵ Their purity was checked by ^{31}P NMR spectroscopy in aqueous solution and by polarography in perchloric acid ethanol–water medium with a rotating glassy carbon electrode for PMo and a mercury dropping electrode for PW.¹⁶ The hydration degree was checked by thermogravimetric analysis.

Anhydrous compounds were obtained by treatment under a nitrogen flow of 500 mg of finely ground hydrated acid ($13H_2O$ hydrate) in a thermal analysis apparatus (Sartorius electro balance). Temperature was slowly increased up to the range stability of anhydrous compounds (200 °C for PMo and 250 °C for PW) and the water loss was measured during the dehydration process. Samples were then left for 2 h at this temperature until no supplementary loss of water was observed. Then they were cooled at room temperature under nitrogen flow and transferred into a desiccator under argon atmosphere. Rotors were then filled with anhydrous samples in a vacuum box, under argon flow.

NMR Measurements. Static, one-pulse MAS and REDOR-MAS NMR experiments were performed on a Bruker ASX 400 spectrometer equipped with a Bruker MAS double resonance probe with 4 mm o.d. rotors at Larmor frequencies of 161.9 MHz for ^{31}P and 400 MHz for 1H . The spinning speed (12–15 kHz) was stabilized to within ± 2 Hz by using a Bruker spinner control unit. Taking into account the frictional heating due to MAS speed,¹⁷ the sample temperature in the REDOR experiments was always between 306 and 315 K. For static and one-pulse MAS experiments, a $\pi/2$ pulse with a recycle delay of 3 s for 1H and 30 s for ^{31}P was used. 1H MAS spectra were also recorded at 14.1 T on a Bruker AVANCE 600 spectrometer for comparison with 400 MHz spectra. 1H and ^{31}P chemical shifts were referenced to TMS and orthophosphoric acid, respectively. REDOR experiments were performed by using the pulse sequence shown in Figure 1. A XY-4 phase cycling

(12) Fournier, M.; Feumi-Jantou, C.; Rabia, C.; Herve, G.; Launay, S. *J. Chem. Mater.* **1992**, 2, 971 and references therein.

(13) (a) Kozhevnikov, I. V.; Sinnema, A.; Jansen, R. J. J.; van Bekkum, H. *Mendeleev. Commun.* **1994**, 92. (b) Kozhevnikov, I. V.; Sinnema, A.; Jansen, R. J. J.; van Bekkum, H. *Catal. Lett.* **1994**, 27, 187. (c) Kozhevnikov, I. V.; Sinnema, A.; Jansen, R. J. J.; van Bekkum, H. *Catal. Lett.* **1995**, 34, 213.

(14) Kozhevnikov, I. V.; Sinnema, A.; van Bekkum, H.; Fournier, M. *Catal. Lett.* **1996**, 41, 153.

(15) Rocchiccioli-Deltcheff, C.; Fournier, M.; Franck, R.; Thouvenot, R. *Inorg. Chem.* **1983**, 22, 207.

(16) Massart, R.; Hervé, G. *Rev. Chim. Miner.* **1968**, 5, 506.

(17) Grimmer, A. R.; Kretschmer, A.; Cajipe, V. B. *Magn. Reson. Chem.* **1997**, 35–2, 86.

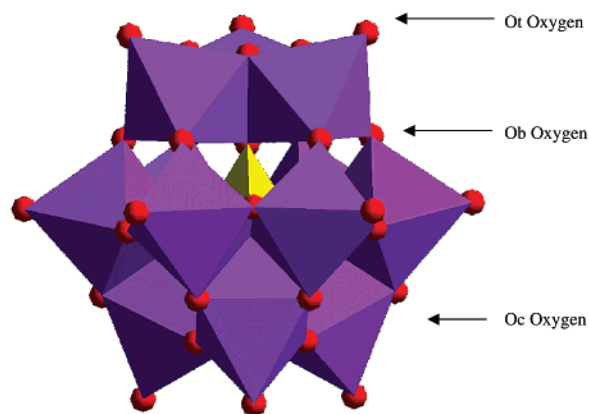


Figure 2. Localization of the oxygen atoms in a PMo^{3-} Keggin structure: oxygen in red, molybdenum in purple, and phosphorus in yellow. The O_a type of oxygen atoms is not observable in this figure.

for I spin π pulses¹⁸ with rf fields of 100 kHz was employed. Two independent REDOR experiments were performed, one for the ^1H observation [$^1\text{H}\{^{31}\text{P}\}$ REDOR] and the other for the ^{31}P observation [$^{31}\text{P}\{^1\text{H}\}$ REDOR]. In each of these experiments, the normalized REDOR fraction, defined as $\Delta S/S_0$, was measured and plotted as a function of the dipolar dephasing time NT_r , T_r being the rotor period.

III. “Ab Initio” DFT Calculations

All calculations have been made with the ADF density functional program.¹⁹ To improve the numerical accuracy of the calculations, we have included GGA corrections.^{20–22} As the structures involve highly charged anions, we added polarization functions in the basis set (triple- ζ and polarization) for oxygen and hydrogen elements. The frozen core approximation has been used to reduce the large computational effort. These cores include all orbitals up to the 3d for the molybdenum atom, the 2p for the phosphorus atom, the 4d for the tungsten atom and the 1s for the oxygen atom. Calculations on the $\text{PW}_{12}\text{O}_{40}^{3-}$ ion (PW^{3-}) include the scalar relativistic effect via a frozen core potential. The total accuracy of the calculations should be better than 0.1 eV. For comparison with experimental REDOR measurements, one should keep in mind that these calculations are performed in the gas phase, while NMR experiments are performed in the crystal phase. Results on the two phases should be quite similar but small differences due to the general electrostatic field should not be excluded.

Keggin anions are constituted by the assembly of corner-shared octahedra from trimetallic groups around a heteroatom (phosphorus) tetrahedron. Each trimetallic group exhibits edge-sharing octahedra (Figure 2). In each trimetallic group, the μ_2 -oxo bridges are usually named O_c , while the μ_2 -oxo bridges linking the trimetallic groups are named O_b . The μ_4 -oxo bridges between the central tetrahedron and the trimetallic groups are named O_a . The fourth type of oxygen atom, the terminal one, only bounded to one metallic atom is named O_t .

First, we have optimized the two ionic Keggin structures (PMo^{3-} and PW^{3-}). The computed distances and angles are in good agreement with the crystallographic data (Table 1). During the geometric optimization, the symmetry of PMo^{3-} is reduced from T_d to T . Indeed, the $\text{Mo}-\text{O}_c$ distances are not equal inside

Table 1. Comparison of the Calculated and Experimental Geometrical Parameters

	PMo^{3-}		PW^{3-}	
	calcd	exptl ^a	calcd	exptl ^b
$\text{M}-\text{O}_t$ (pm)	173	168	170	170
$\text{M}-\text{O}_c$ (pm)	≈ 194	≈ 191	190	191
$\text{M}-\text{O}_b$ (pm)	192	192	188	190
$\text{M}-\text{O}_c-\text{M}$ (deg)	124	125	125	126
$\text{M}-\text{O}_b-\text{M}$ (deg)	152	151	152	152

^a References 23 and 24. ^b References 24 and 25.

Table 2. Mulliken Charge of the Electron from DFT Calculations

atom	PMo^{3-}	PW^{3-}
O_b	−0.86	−1.00
O_c	−0.89	−1.07
O_t	−0.64	−0.74
Mo	+2.28	
W		+2.70

the four Mo_3O_{10} trimers. Precise diffraction analyses indicate that these distances take alternatively two values: 185 and 196 pm. Our calculations reproduce this periodic succession of relatively short and relatively long distances in the MoO_6 unit as evidenced in crystallographic data. Our calculations show that the PW^{3-} Keggin structure has the perfect T_d symmetry, in conformity with the diffraction data, but as an unexpected result considering the literature, the PW^{3-} structure appears more ionic than that of PMo^{3-} . The Mulliken charges are summarized in Table 2. In the fully ionic description, the formal charge of the metallic center is +6e but the computed ones are only +2.70e for the tungsten and +2.28e for the molybdenum. Within the two structures, the less charged oxygen atom is O_t , as expected from the usual double bond description. The differences between the two kinds of bridging oxygen atoms, O_b and O_c , are small (0.03e and 0.07e for PMo^{3-} and PW^{3-} respectively).

In contrast, the highly occupied molecular orbital (HOMO) and the lower unoccupied molecular orbital (LUMO) of the two structures are very similar. The HOMO is mainly localized on the bridging oxygen atoms while the LUMO is localized on the metal atoms.^{26,27} These LUMO are almost purely nonbonding, doubly degenerate, and this explains why it is so easy to introduce four electrons by groups of one or two, depending on the pH, in a quasireversible process.^{2,16} This is likely to be the reason for the good efficiency in many oxydehydrogenation reactions which need bi-electronic exchange between the catalyst and the substrate.

Second, we have computed the proton affinity (PA) of the various sites of the PMo and PW Keggin structures. A previous work suggested that the more stable position for the first proton is a bridged one for the two kinds of Keggin structures.²⁸ However, these calculations have been performed on one part of the structure and only one site has been studied on the whole Keggin unit. To compare the calculations with the NMR experimental results, we need accurately determined $R_{\text{P-H}}$ distances and hence one must take into account the whole HPAs.

- (18) Gullion, T.; Schaeffer, J. J. *Magn. Reson.* **1991**, 92, 439.
 (19) Baerends, E. J. et al. *Chem. Phys.* **1973**, 2, 41.
 (20) Becke, A. D. *Phys. Rev. A* **1988**, 38, 3098.
 (21) Becke, A. D. *ACS. Symp. Ser.* **1989**, 394, 165.
 (22) Perdew, J. P. *Phys. Rev. B* **1986**, 33, 8822.

- (23) Strandberg, R. *Acta Chem. Scand. A* **1975**, 29, 359.
 (24) Brown, G. M.; Noe-Spirlet, M. R.; Busing, W. R.; Levy, H. A. *Acta Crystallogr. Sect. B* **1997**, 33, 1038.
 (25) Noe-Spirlet, M. R.; Brown, G. M.; Busing, W. R.; Levy, H. A. *Acta Crystallogr. Sect. A* **1975**, 31, S80.
 (26) Lopez, X.; Maestre, J. M.; Bo, C.; Poblet, J. M. *J. Am. Chem. Soc.* **2001**, 123, 9571.
 (27) Taketa, H.; Katsuki, S.; Eguchi, K.; Seiyama, T.; Yamazoe, N. *J. Phys. Chem.* **1986**, 90, 2959.
 (28) Bardin, B. B.; Bordawekar, S. V.; Neurock, M.; Davis, R. J. *Phys. Chem. B* **1998**, 102, 10817.

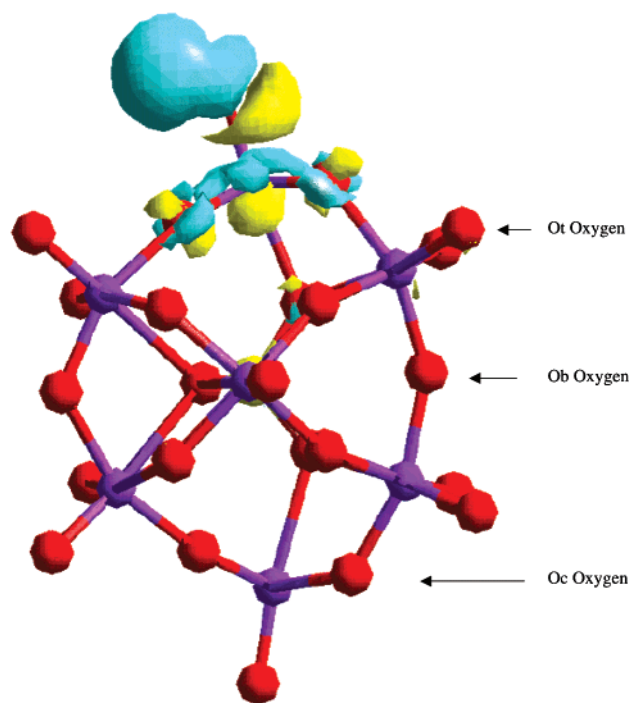
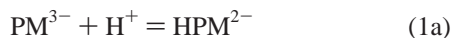


Figure 3. Electron density variation induced by the proton binding to one O_t oxygen atom in a PMo^{3-} structure: the increase in electron density is shown in blue and the decrease in electron density is shown in yellow color.

The proton affinity is related to the variation of energy of reaction 1 corresponding to the last acidity of the Keggin anion ($M = W$ or Mo):



$$PA = E(HPM^{2-}) - E(H^+) - E(PM^{3-}) \quad (1b)$$

For the two systems, the three $HPM_{12}O_{40}^{2-}$ anions are completely optimized geometrically. From this point of view, the distortions induced by the proton are localized in the vicinity of the binding site. Indeed, the second neighbors are only slightly displaced, even for the addition on the bridging sites. From the electronic point of view, the situation is very similar as shown by the variation of the electronic density. The oxygen atom mostly provides the electrons involved in the creation of the OH bond, whatever may be its type. For example, in PMo^{3-} the creation of the O_t-H bond corresponds to the transformation of the $Mo=O_t$ double bond into a single one (Figure 3). The variations on the first and second neighboring atoms are small, and they are negligible on the other parts of the Keggin structure. With these considerations, the DFT calculations have been performed, but limited to the localization of the first proton (HPM^{2-}) in order to reduce the computational effort. Indeed, the number of geometries, which should be tested to determine the relative position of the three protons, is very important, and a priori choices are difficult to justify. However, if the protons are situated on different trimer units, their localization should be similar, as the geometric and electronic deformations induced by the first proton on a second trimer are very small.

The PAs for the (HPM^{2-}) anions are summarized in Table 3. To compare our calculations with the REDOR results, we have also reported the R_{P-H} distances. Between both anions, energy differences between the two bridging oxygen atoms are

Table 3. Calculated Proton Affinity (eV) and R_{P-H} Distance (pm) for the $HPMo^{2-}/HPW^{2-}$ Anions

binding site	PA	R_{P-H}
O_b	-17.2/-16.5	334/348
O_c	-17.0/-16.7	481/466
O_t	-16.4/-16.2	561/586

small (0.2 eV) and the electrostatic field created by the other ions in the crystal could reverse the order of the calculated PAs between the O_b and O_c sites.

Considering now the evolution between the two structures, the PA difference is only 0.2 eV for the O_t atom, while it is larger for the bridging oxygens. This behavior is consistent with the Mulliken charges. Indeed, the charge difference between the two anions is larger for the bridging atoms (0.14e for O_b and 0.18e for O_c) than for the O_t atoms (0.10e).

The creation of hydrogen bonds between two different Keggin anions is an effect that can contribute to the localization of the proton.²⁹ From geometrical considerations, this weak bond is only possible between one O_t oxygen atom and one proton on a second terminal oxygen. Considering the charge of the oxygen atoms and the PA differences, the H bond is more likely to change the energetic order in the PW system than in the PMo one.

The effect of the crystal field could also be an important parameter in this study. To estimate this effect, we have performed test calculations including an external electric field. These tests on the deprotonated PMo^{3-} and PW^{3-} Keggin structures demonstrate that the charges on the O_b and O_c oxygen atoms and on the metallic atoms do not change a lot, while the charge on the O_t atoms is decreased. So, the effect of the crystal field will be much more important on the O_t sites than on the bridging ones. As the energetic differences between the various sites are small on the HPW^{2-} anions, an inversion of the stability order deduced from the DFT calculation cannot be totally excluded.

IV. NMR Results

Magic Angle Spinning (MAS) NMR experiments allow the resonances corresponding to the various proton or phosphorus sites in HPAs to be resolved. Unfortunately, however, the dipolar interaction between the proton and phosphorus is averaged to zero by MAS. Owing to an inverse cube relationship that internuclear distances have on the dipolar interactions, their determination is nevertheless mandatory for structural purposes, thus emphasizing the analysis of proton-phosphorus distances in HPAs.

The REDOR technique was originally proposed by Gullion and Schaefer to recouple the heteronuclear dipolar coupling between an isolated I-S spin pair.^{30,31} Although this interaction, which we seek to measure, is removed by MAS, it is suitably recoupled by the application of rotor synchronized π pulses on the dipolar coupled I spins, applied twice per rotor period, with a single S spin π pulse applied halfway during the sequence. The net propagation of this dipolar evolution can be conveniently chosen to last over a sequentially incremented number $N = 2(n + 1)$ of dephasing rotor periods T_r . In the actual experiment, a

(29) Day, V. W.; Klemperer, W. G.; Maltbie, D. J. *J. Am. Chem. Soc.* **1987**, *109*, 2991.

(30) Gullion, T.; Schaefer, J. J. *Magn. Reson.* **1989**, *81*, 196.

(31) Gullion, T.; Schaefer, J. *Adv. Magn. Reson.* **1989**, *13*, 57.

control signal $S_0(N\tau_r)$ and a dipolar dephased signal $S(N\tau_r)$ are recorded in two separate experiments by removing and including respectively the I spin π pulses. This allows an estimation of the normalized REDOR fraction:

$$\Delta S/S_0(N\tau_r) = 1 - S(N\tau_r)/S_0(N\tau_r) \quad (2)$$

which depends on the dipolar couplings $D = \gamma_P\gamma_H/R_{\text{P-H}}^3$. These couplings only contain the proton–phosphorus distance $R_{\text{P-H}}$, and the gyromagnetic ratios γ_P and γ_H . In the case of one isolated spin pair (proton–phosphorus in HPAs), the analytical expression describing the REDOR evolution of powder samples can be written:³⁰

$$S(N\tau_r) = 1/4\pi \int \int \cos[\sqrt{2}DN\tau_r \sin 2\beta \sin \alpha/\pi] \sin \beta \, d\beta \, d\alpha \quad (3)$$

where polar angles (α, β) describe the rotor axis with respect to the P-H vector.

In HPAs, each phosphorus atom is dipolar coupled with three protons. In the case where proton–proton interactions are negligible, the phosphorus REDOR signal can thus be written³²

$$S(N\tau_r) = 1/8\pi^2 \int \prod \cos[\sqrt{2}D^i N\tau_r \sin 2\beta^i \sin \alpha^i/\pi] \, d\Omega \quad (4)$$

This powder averaging must take into account the relative orientations of the three different vectors P-H^i . It has recently been shown that a new type of selective REDOR experiment can be used to select at will isolated spin pairs in multispin systems.³³ However, this method requires that differences of chemical shifts are observed in the MAS spectrum and this does not apply to HPAs. In the case where these three protons experience fast chemical exchange, the previous formulas must be transformed into:

$$S(N\tau_r) = 1/8\pi^2 \int \cos[\sum \sqrt{2}D^i N\tau_r \sin 2\beta^i \sin \alpha^i/\pi] \, d\Omega \quad (5)$$

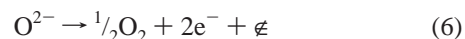
(a) $\text{H}_3\text{PW}_{12}\text{O}_{40}$. The ^1H MAS spectrum (Figure 4a) exhibits a single broad resonance at 8.9 ppm, which is due to the normal Keggin structure with three isolated protons. This result is in accordance with that of Uchida et al. for anhydrous $\text{H}_3\text{PW}_{12}\text{O}_{40}$ compound.³⁴ The ^{31}P MAS spectrum (Figure 4b) displays two peaks: one narrow ($\Delta\nu = 160$ Hz) minor (22%) one at -10.8 ppm and one broader ($\Delta\nu = 275$ Hz) major (78%) one at -12.0 ppm. Even if in this Keggin compound the phosphate group can be considered to be isolated (as indicated by vibrational spectrometry¹⁵), it is generally admitted that,^{35–38} in the solid state, phosphorus resonances are very sensitive to the crystal structure. This observation is in agreement with respect to that of Essayem et al. for dehydration at 250°C .³⁵ These authors suggest that two competitive secondary structures, cubic and quadratic, exist around this dehydration temperature. So, the narrow weak resonance at -10.8 ppm could be ascribed to a

well-crystallized anhydrous phase, while the broader line at -12.0 ppm could be ascribed to an “amorphous” phase. The distribution of surroundings corresponding to the “amorphous” phase is evidenced by the fact that this resonance presents a constant line width of 1.7 ppm, independent of the static magnetic field (9.4 and 14 T). The REDOR experiments have been performed on this major signal.

The experimentally determined REDOR evolutions for the $^1\text{H}\{^{31}\text{P}\}$ and $^{31}\text{P}\{^1\text{H}\}$ experiments are shown in Figure 5. Consequent to the fact that each Keggin unit contains only one phosphorus atom, one can consider that the $^1\text{H}\{^{31}\text{P}\}$ REDOR evolution (Figure 5A) is describable by an isolated spin pair approximation. By fitting the experimental data points using eq 3, we obtain for the best estimate $R_{\text{P-H}} = 570 \pm 20$ pm.

On the contrary, for the $^{31}\text{P}\{^1\text{H}\}$ REDOR behavior (Figure 5B), we must take into account simultaneously the three phosphorus–proton vectorial dipolar couplings (eq 4). To simplify calculations, we have assumed that the three protons lie in the same plane as the phosphorus atom and the three corresponding P–H distances are the same. By fitting the experimental data points, we obtain the same distance estimate ($R_{\text{P-H}} = 570 \pm 20$ pm). Clearly, this estimate is very different from the result one obtains ($R_{\text{P-H}} = 480$ pm) by assuming one isolated spin-pair (see Figure 5B). In the framework of this planar description, the proton–proton distance is ca. 1000 pm, which rules out the possibility of fast chemical exchange. Further, if the proton exchange occurs, there should be no $^{31}\text{P}\{^1\text{H}\}$ REDOR evolution according to eq 5. This is also in accordance with the nonnegligible ^1H static line width (5 kHz).

(b) $\text{H}_3\text{PMo}_{12}\text{O}_{40}$. In distinct contrast to the PW spectra, the ^1H MAS spectrum of PMo exhibits three different resonances at 5.6, 7.1 and 12.2 ppm (Figure 4a). However, as in the PW compound, a slight amorphous character is indicated by the small chemical shift distribution and is duly supported by the poor XRD data. As the crystal symmetries of these two anhydrous compounds are very similar,¹² it seems reasonable to ascribe these signals to three separate microphases. One of them, the major intense signal at 7.1 ppm, could be ascribed to the normal $\text{H}_3\text{PMo}_{12}\text{O}_{40}$ anhydrous phase. However, the solid seems to be slightly reduced during the thermal treatment as its color turns green from yellow. ESR measurements performed at 77 and 300 K confirm the existence of mobile electrons associated with some paramagnetic species having very fast relaxation. Consequently, one of the other signals should be ascribed to a proton shifted by paramagnetic effect in an amorphous phase. The reduction process has to be induced by a partial thermal decomposition of the molybdenum Keggin unit, more reactive than the tungsten one, as indicated previously.³⁹ That kind of evolution occurs from the lost oxygen atom, leading to a two-electron reduced compound and a vacancy according to the well-admitted scheme in oxo compounds:⁴⁰



These reduced molybdenum Keggin units can be ascribed to the less intense and paramagnetically shifted (to low field) broad resonance observed at 12.2 ppm. Indeed, independent ^1H – ^1H

(32) Goetz, J.; Schaefer, J. *J. Magn. Reson.* **1997**, *127*, 147.

(33) Jaroniec, C. P.; Tounge, B. A.; Herzfeld, J.; Griffin, R. G. *J. Am. Chem. Soc.* **2001**, *123*, 3507.

(34) Uchida, S.; Inumara, K.; Misono, M. *J. Phys. Chem. B* **2000**, *104*, 8108.

(35) Essayem, N.; Tong, Y. Y.; Jobic, H.; Vedrine, J. C. *Appl. Catal. A* **2000**, *194–195*, 109.

(36) Essayem, N.; Kieger, S.; Coudurier, G.; Fournier, M.; Vedrine, J. C. *Catal. Lett.* **1995**, *34*, 223.

(37) Black, J. B.; Clayden, N. J.; Gai, P. L.; Scott, J. D.; Servick, E. M.; Goodenough, J. B. *J. Catal.* **1987**, *106*, 1.

(38) Okuhara, T.; Nishimura, T.; Watanabe, H.; Misono, M. *J. Mol. Catal.* **1992**, *74*, 247.

(39) Paze, C.; Bordiga, S.; Zecchina, A. *Langmuir* **2000**, *16*, 8139.

(40) Blouet-Crussan, E.; Rigole, M.; Fournier, M.; Aboukais, A.; Daubrege, F.; Hecquet, G.; Guelton, M. *Appl. Catal. A* **1999**, *178*, 69 and references therein.

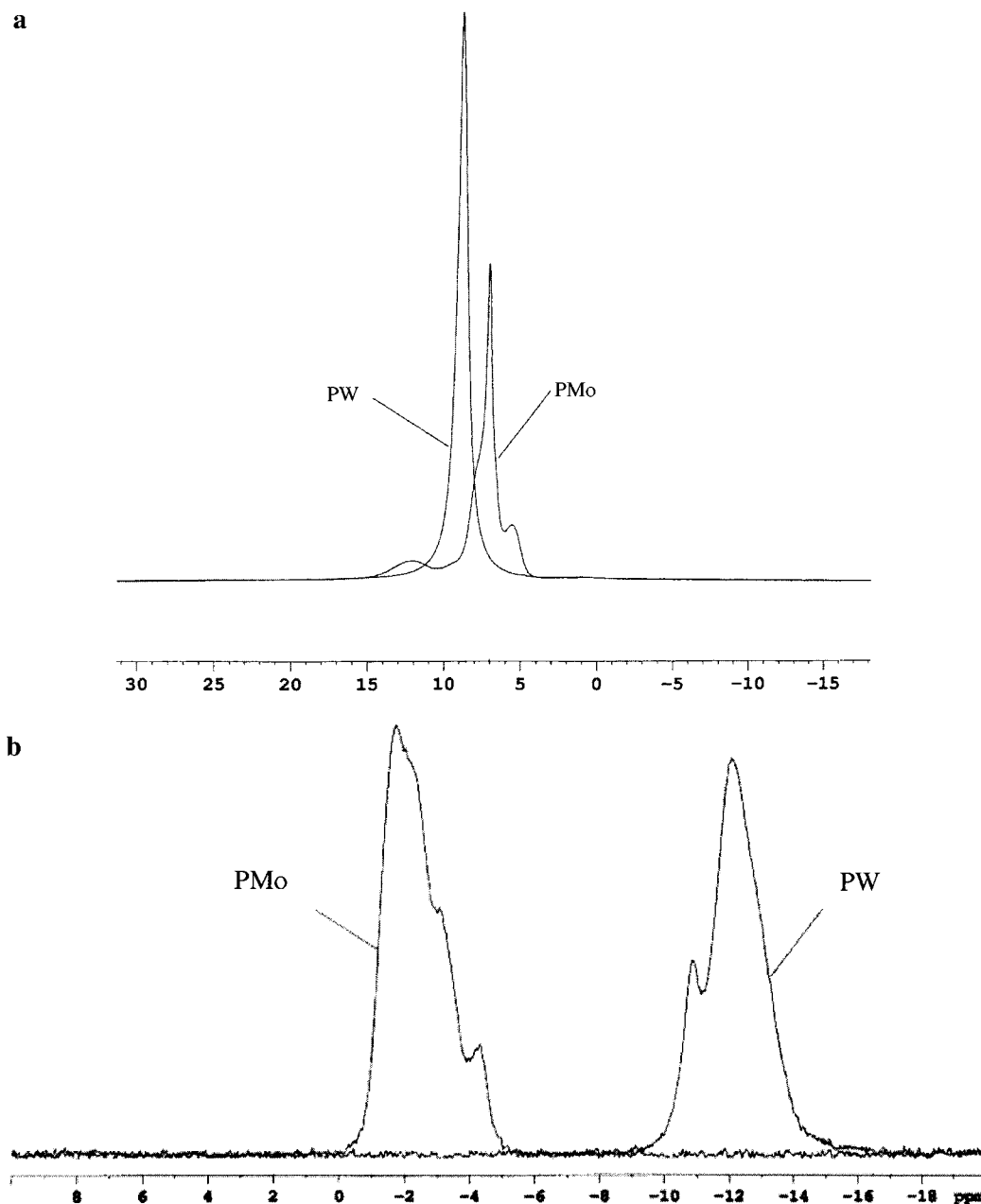
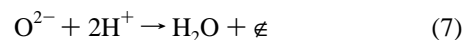


Figure 4. ^1H (a) and ^{31}P (b) MAS NMR spectra of $\text{H}_3\text{PMo}_{12}\text{O}_{40}$ and $\text{H}_3\text{PW}_{12}\text{O}_{40}$ recorded at a spinning speed of 15 kHz.

2D exchange experiments conducted with mixing times up to 200 ms clearly indicated the absence of any exchange cross-peak between the 12.2 ppm signal and the signals at 5.6 and 7.1 ppm (see the Supporting Information). This clearly shows that this resonance belongs to a separate microphase. Moreover, proton spin–lattice relaxation experiments show that its T_1 value (740 ms) is shorter than the relaxation times (900 ms and 1.1 s) measured for the other two signals. This reduction in T_1 value is in accordance with the ESR measurements and supports our view that the 12.2 ppm proton signal arises from the reduced Keggin units which are paramagnetic in nature. Theoretically, the two electrons should present diamagnetic coupling in the reduced Keggin unit, but their mobility may explain the small paramagnetic effect observed on the localized protons.⁴¹

Another pathway can also occur, in which the vacancy can be created from the oxo ion and proton departure through the water molecule formation according to the following scheme:



This second process, which occurs without reduction (hence is not paramagnetic), could explain the minor line at 5.6 ppm, and in this case the remaining proton appears to be more strongly attached on the Keggin ion. Although this can be identified as a different kind of Keggin unit, ^1H – ^1H 2D exchange experiments show that there is a strong spin–spin interaction between these Keggin units and the normal Keggin units, suggesting that there is more mixing at the molecular level between these two different microphases (see the Supporting Information).

Another strong argument to support the existence of three such types of anhydrous Keggin units in the solid is that the

(41) Fournier, M.; Rocchiccioli-Deltcheff, C.; Kazansky, L. P. *Chem. Phys. Lett.* **1994**, *223*, 297.

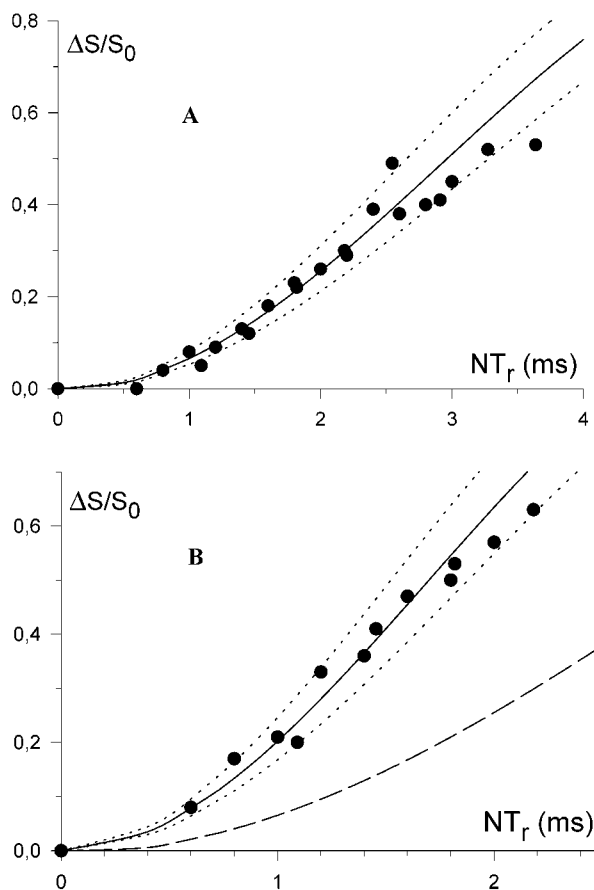


Figure 5. $^1\text{H}\{^{31}\text{P}\}$ REDOR (A) and $^{31}\text{P}\{^1\text{H}\}$ REDOR (B) results of $\text{H}_3\text{-PW}_{12}\text{O}_{40}$. The experimental data points are denoted by the solid circle. The simulated curve (solid line) was calculated in the manner discussed in the text, using an internuclear distance of $R_{\text{P-H}} = 570$ pm. The dotted lines were calculated by changing this distance by ± 20 pm. The dashed line in part B shows the result obtained by considering only one isolated H–P spin pair, with a $R_{\text{P-H}}$ distance of 570 pm.

$^1\text{H}\{^{31}\text{P}\}$ REDOR evolutions are markedly different for the three proton signals in PMo (Figure 6A). This leads to different $R_{\text{P-H}}$ distance estimates for the primary Keggin units in each of the three distinctly different domains evidenced by the proton spectrum: normal, reduced (departure of oxygen) and dehydrated (departure of the constitution water molecule) Keggin units. For the primary structure of the normal Keggin ion, we focus our attention on the REDOR evolution for the main signal at 7.1 ppm and from eq 3 we determine $R_{\text{P-H}} = 520 \pm 20$ pm. This value is noticeably shorter for the Keggin units in the reduced microphase ($R_{\text{P-H}} \approx 490$ pm) and in the dehydrated microphase ($R_{\text{P-H}} \approx 460$ pm).

For the $^{31}\text{P}\{^1\text{H}\}$ REDOR (Figure 6B), we employ the multispin description, as we have used for PW, and determine the same proton–phosphorus distance $R_{\text{P-H}} = 520 \pm 20$ pm for the normal Keggin units. However, if we assume an isolated spin pair (eq 3), the proton–phosphorus distance determined from $^{31}\text{P}\{^1\text{H}\}$ REDOR ($R_{\text{P-H}} = 440 \pm 20$ pm) is much shorter than the one determined from $^1\text{H}\{^{31}\text{P}\}$ REDOR. As in the case of PW, we rule out the possibility of fast proton chemical exchange (eq 5) in PMo, due to the fact that the observed $^{31}\text{P}\{^1\text{H}\}$ REDOR curve is not completely flat. This is also in accordance with the large ^1H static line width (≈ 6 kHz).

A comparison of the proton chemical shifts (Figure 4a) corresponding to the two anhydrous normal phases of PW and

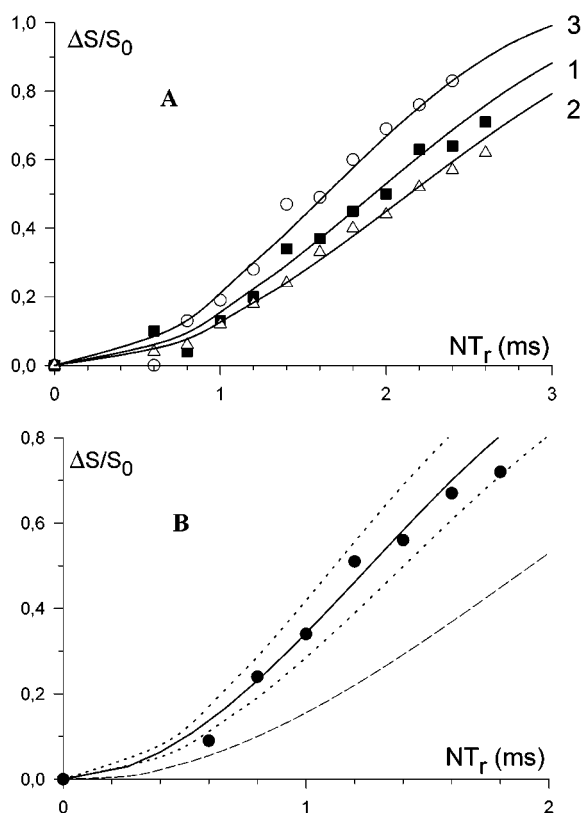


Figure 6. (A) $^1\text{H}\{^{31}\text{P}\}$ REDOR curves of $\text{H}_3\text{PMo}_{12}\text{O}_{40}$. The simulated curves (solid line) were obtained for internuclear $R_{\text{P-H}}$ distances of 490 (1: 12.2 ppm), 520 (2: 7.1 ppm) and 460 pm (3: 5.6 ppm). (B) $^{31}\text{P}\{^1\text{H}\}$ REDOR curves of $\text{H}_3\text{PMo}_{12}\text{O}_{40}$. The simulated curve (solid line) was obtained for an internuclear distance of $R_{\text{P-H}} = 520$ pm. The dotted lines were calculated by changing $R_{\text{P-H}}$ by ± 20 pm. The dashed line was obtained by considering one isolated P–H spin pair, with $R_{\text{P-H}} = 520$ pm. The experimental data points are denoted by the following symbols: 1, ■; 2, △; and 3, ○.

PMo (8.9 and 7.1 ppm, respectively) clearly shows that PW remains more acidic than PMo in its anhydrous form since the shielding of the proton is usually linked to a weaker acidity. Of course, the number of different ^{31}P peaks (Figure 4b) is also larger for PMo than for PW, due to the existence of three separate microphases for this compound which are also indicated by the ^1H NMR spectrum. A comparison of the phosphorus chemical shifts (PMo ≈ -2 ppm and PW ≈ -12 ppm) shows that they may be correlated with the ionic character of the metal–oxygen bond (Table 2). The more charged the oxygen atoms are, the more important the diamagnetic shielding of the Keggin unit at its center is. Then the small charge changes of oxygen atoms which occur in the oxygen vacancy formation for PMo will also involve the existence of several ^{31}P MAS signals.

V. Comparison of REDOR Results and DFT Calculations

The $R_{\text{P-H}}$ distances derived from REDOR experiments are compared for PMo and PW with distance estimates provided by DFT calculations for the different proton locations at O_b , O_c , and O_t sites.

From the DFT calculations, the localization of the proton on the PW^{3-} anion remains ambiguous. Indeed, the energetic differences between the three computed PAs are too small to clearly pinpoint the proton location. This ambiguity is removed by our REDOR experiments. Quite significantly, when the

related distance estimate ($R_{\text{P-H}} = 570 \pm 20$ pm) derived from $^1\text{H}\{^{31}\text{P}\}$ and $^{31}\text{P}\{^1\text{H}\}$ REDOR experiments is compared with those provided by DFT calculations, the proton location is unambiguously determined to be at the terminal O_t position. This location is in agreement to that deduced from infrared data.⁴²

For the PMo compound, the comparison of DFT and REDOR distance estimates locates the protons either on the O_c or on the O_t type of oxygen atoms. However, the proton affinity calculations (Table.3) have shown that the O_t site is definitively the least stable in PMo. Thus, the REDOR results, taken with the DFT calculations, show that the proton location in PMo is at the second bridging oxygen site (O_c). We must also remember that the secondary structure,¹² not taken into account in the DFT calculations, may introduce some small variations of the $R_{\text{P-H}}$ distance.

Conclusions

We have shown that the locations of acidic protons can be determined unambiguously in anhydrous solid acid catalysts by REDOR NMR and DFT quantum chemical calculations. This is especially useful since it is not possible to grow single crystals suitable for X-ray studies. For the two extensively studied heteropolyacid systems $\text{H}_3\text{PMo}_{12}\text{O}_{40}$ and $\text{H}_3\text{PW}_{12}\text{O}_{40}$, the protons are located at a distance of 520 ± 20 and 570 ± 20 pm, respectively, from the central phosphorus of the Keggin anion.

This shows that the acidic sites are the second type (O_c) of bridging oxygen atom in Mo and the terminal oxygen (O_t) atom in the W HPA Keggin structures. Similar REDOR experiments, further aided by DFT quantum chemical calculations, also correlated with classical MAS 1D NMR spectra in a variety of native and isomorphically substituted solid acids thus appear to offer new opportunities to rank the acidity and oxygen lability properties of these classes of important solid Keggin catalysts and correlate with their catalytic performance.

Acknowledgment. The authors thank Mr. B. Revel of the Centre Commun de Mesures RMN (USTL) for help and technical support. Dr J. M. Wieruszewski (Institut de Biologie de Lille) is also acknowledged for the additional ^1H and ^{31}P NMR spectra (AVANCE 600). The authors thank Mrs. C. Guelton for the TG characterization and for the preparation of anhydrous solid and are very grateful to the Region Nord/Pas-de-Calais for purchasing the ASX-400 and AVANCE-600 NMR spectrometers and also for the support extended to one of them (S.G.) as an invited scientist. Some DFT calculations of this study have been performed on the IDRIS CNRS computer center. J.P.A. and S.G. also thank Indo-French Centre for Promotion of Advanced Research, IFCPAR, New-Delhi, for support of project 2105-1.

Supporting Information Available: Sample preparations and 2D exchange spectra (PDF). This material is available free of charge via the Internet at <http://pubs.acs.org>.

JA017848N

(42) Rocchiccioli-Deltcheff, C.; Aoussi, A.; Bettahar, M. M.; Launay, S.; Fournier, M. *J. Catal.* **1996**, *164*, 16.